Mon. Not. R. Astron. Soc. **352,** 1413–1420 (2004) doi:10.1111/j.1365-2966.2004.08032.x

An improved approach to measuring H_0 using X-ray and SZ observations of galaxy clusters

R. W. Schmidt,[1⋆] S. W. Allen[2] and A. C. Fabian[2]
[1]*Institut für Physik, Universität Potsdam, Am Neuen Palais 10, 14469 Potsdam, Germany*
[2]*Institute of Astronomy, University of Cambridge, Madingley Road, Cambridge CB3 0HA*

Accepted 2004 May 14. Received 2004 May 13; in original form 2003 September 1

ABSTRACT

We present an improved method for predicting the Sunyaev–Zeldovich (SZ) effect in galaxy clusters from spatially resolved, spectroscopic X-ray data. Using the deprojected electron density and temperature profiles measured within a fraction of the virial radius, and assuming a Navarro–Frenk–White mass model, we show how the pressure profile of the X-ray gas can be extrapolated to large radii, allowing the Comptonization parameter profile for the cluster to be predicted precisely. We apply our method to *Chandra* observations of three X-ray-luminous, dynamically relaxed clusters with published SZ data: RX J1347.5–1145, Abell 1835 and Abell 478. Combining the predicted and observed SZ signals, we determine improved estimates for the Hubble constant from each cluster and obtain a weighted mean of $H_0 = 69 \pm 8\,\mathrm{km\,s^{-1}\,Mpc^{-1}}$ for a cosmology with $\Omega_\mathrm{m} = 0.3$ and $\Omega_\Lambda = 0.7$. This result is in good agreement with independent findings from the Hubble Key Project and the combination of cosmic microwave background and galaxy cluster data.

Key words: cosmic microwave background – cosmology: observations – distance scale – X-rays: galaxies: clusters.

1 INTRODUCTION

The inverse Compton scattering of cosmic microwave background (CMB) photons by hot electrons in galaxy clusters leads to a distortion of the CMB spectrum along the line of sight, known as the Sunyaev–Zeldovich (SZ, Sunyaev & Zeldovich 1972) effect. The magnitude of the SZ effect is determined by the Comptonization parameter of the cluster gas, $y(r)$, which is proportional to the line-of-sight integral of the gas pressure.

It was recognized swiftly (Silk & White 1978; Cavaliere, Danese & de Zotti 1979) that for an assumed, simple geometry, the combination of X-ray and SZ observations can be used to measure the angular diameter distance to a cluster. The ratio of the observed (based on radio/submillimetre observations) and predicted (based on X-ray observations) SZ signals is proportional to the square root of the angular diameter distance, making this, potentially, an exceptionally powerful technique for probing the cosmic distance scale.

Although the SZ effect is now employed frequently to determine extragalactic distances (e.g. Mauskopf et al. 2000; Carlstrom et al. 2001; Jones et al. 2001; Mason, Myers & Readhead 2001; Reese et al. 2002), most studies to date have relied on the application of the β-model (Cavaliere & Fusco-Femiano 1978) in their X-ray analyses. The β-model provides a simple analytical approximation to the spatial distribution of the cluster gas. These studies have also generally assumed isothermality and relied on broad-beam measurements of the mean, emission-weighted temperature when calculating the gas pressure.

With the *Chandra* X-ray Observatory and *XMM–Newton* it is now possible to measure the temperature, density and pressure profiles of the cluster gas precisely. The surface brightness distribution, in particular, can be resolved on subarcsecond scales. *Chandra* observations have shown that β-models do not, generally, provide good descriptions of the X-ray gas distributions in the cores of dynamically relaxed clusters, and that the gas temperature is not isothermal but drops sharply within cluster cores (e.g. Allen, Schmidt & Fabian 2001b; Schmidt, Allen & Fabian 2001; Kaastra et al. 2004). The main limitation of the new X-ray observations is that (due to background levels and restricted fields of view; 8×8 arcmin^2 for the *Chandra* ACIS-S detector) the gas temperature can only be measured directly out to radii $r \lesssim$ one-third of the virial radius for most clusters. Since predictions of the SZ effect require the line-of-sight pressure integral through the cluster, extrapolation of the X-ray results is therefore required for combined X-ray/SZ work.

In this paper we present a recipe for calculating the predicted SZ effect in clusters which makes use of the spatially resolved spectroscopic techniques described in our earlier work, and which includes a new method for extrapolating the X-ray pressure profiles beyond

⋆E-mail: rschmidt@astro.physik.uni-potsdam.de

the directly observed region. Analytical formulae for the electron density and temperature profiles of the X-ray gas at large radii are obtained under the assumption of hydrostatic equilibrium. These can be computed easily and used for SZ analysis. We show that our method, which takes full account of the observed density and temperature profiles of the X-ray-emitting gas, provides a significant improvement in accuracy with respect to the standard isothermal β-model.

The outline of this paper is as follows. In Section 2 we review the standard β-model approach and describe our improved method. In Section 3 we apply our method to *Chandra* X-ray and SZ observations of three highly X-ray-luminous, dynamically relaxed galaxy clusters: RX J1347.5–1145 ($z = 0.451$), Abell 1835 ($z = 0.2523$) and Abell 478 ($z = 0.088$). In Section 4 we use the combined data to measure the Hubble constant. In Section 5 we compare our results to those obtained using the standard isothermal β-model approach. A summary of the results can be found in Section 6.

Unless stated otherwise, all quantities are quoted for a Hubble constant $H_0 = 70\,\mathrm{km\,s^{-1}}$ Mpc^{-1}, matter density $\Omega_\mathrm{m} = 0.3$ and vacuum energy density $\Omega_\Lambda = 0.7$. Error bars correspond to 1σ (68.3 per cent) confidence.

2 PREDICTING THE SZ EFFECT

2.1 The standard β-model approach

Within the context of the isothermal β-model (Cavaliere & Fusco-Femiano 1978), the surface brightness profile of a galaxy cluster can be written as

$$I(\theta) \propto \left[1 + \left(\frac{\theta}{\theta_\mathrm{c}}\right)^2\right]^{-3\beta+\frac{1}{2}}, \tag{1}$$

where θ_c is the angular core radius and β is the slope parameter. By calculating the X-ray emission due to hot cluster gas at a temperature T (e.g. Kaastra & Mewe 1993; Liedahl et al. 1995), one can invert this to yield the central electron density $n_{\mathrm{e}0}$ of the corresponding intrinsic (three-dimensional) electron density profile

$$n_\mathrm{e}(r) = n_{\mathrm{e}0}\left[1 + \left(\frac{r}{r_\mathrm{c}}\right)^2\right]^{-\frac{3\beta}{2}}, \tag{2}$$

where the core radius r_c follows from the angular diameter distance d of the cluster, $r_\mathrm{c} = d\theta_\mathrm{c}$.

The Comptonization parameter along a line of sight at an impact parameter R is defined by

$$y(R) = \frac{2\,\sigma_\mathrm{T}\,k_\mathrm{B}}{m_\mathrm{e}\,c^2}\int_R^\infty \frac{n_\mathrm{e}(r)\,T(r)}{\sqrt{r^2 - R^2}}\,r\,\mathrm{d}r \tag{3}$$

(e.g. Birkinshaw 1999, where we have converted the equation into an integral along radius r). Here σ_T is the Thomson cross-section, k_B the Boltzmann constant, c the speed of light, and m_e the electron mass. Equation (3) can be integrated analytically for the isothermal β-model (e.g. Birkinshaw 1999) to give

$$y(R) = y_0\left[1 + \left(\frac{R}{r_\mathrm{c}}\right)^2\right]^{-\frac{3}{2}\beta+\frac{1}{2}}, \tag{4}$$

with the normalization constant

$$y_0 = n_{\mathrm{e}0}\,r_\mathrm{c}\,\sigma_\mathrm{T}\left(\frac{k_\mathrm{B}T}{m_\mathrm{e}c^2}\right)B\left(\frac{1}{2}, \frac{3\beta}{2} - \frac{1}{2}\right) \tag{5}$$

(Mauskopf et al. 2000), where $B(a, b) = \Gamma(a)\,\Gamma(b)/\Gamma(a + b)$ is the beta function.

In previous work, the temperature T has usually been taken to be the mean emission-weighted temperature of the X-ray gas, determined with broad-beam instruments. However, as discussed in Section 1, observations with the *Chandra* and *XMM–Newton* satellites have shown that regular, dynamically relaxed galaxy clusters are not isothermal. This temperature variation should be accounted for in the analysis.[1]

Finally, clusters are not infinitely large, as is usually assumed when calculating the predicted Comptonization parameter profile using the β-model. In what follows we show how modern X-ray data can be used to integrate equation (3) without the assumption of isothermality, taking account of the finite size of galaxy clusters. In particular, where the region of the cluster directly observed in X-rays is small, the use of an extrapolation procedure like the one described here can become important.

2.2 An improved approach

2.2.1 Discretization of the *y*-parameter calculation

In order to calculate the expected y-parameter profile (equation 3) for a particular galaxy cluster, the temperature profile $T(r)$ and the electron density profile $n_\mathrm{e}(r)$ need to be known. In practice, deprojection analyses of *Chandra* or *XMM–Newton* data (e.g. Schmidt et al. 2001, and references therein) provide the electron density and X-ray gas temperature in N discrete shells, with inner and outer radii $r_{\mathrm{in},i}$ and $r_{\mathrm{out},i}$, respectively. We can thus recast equation (3) into a sum starting with shell j at impact parameter R:

$$y(R) = \frac{2\,\sigma_\mathrm{T}\,k_\mathrm{B}}{m_\mathrm{e}\,c^2}\left[n_{\mathrm{e,j}}\,T_\mathrm{j}\sqrt{r_{\mathrm{out,j}}^2 - R^2} + \sum_{i=\mathrm{j}+1}^{N} n_{\mathrm{e},i}\,T_i\left(\sqrt{r_{\mathrm{out},i}^2 - R^2} - \sqrt{r_{\mathrm{in},i}^2 - R^2}\right)\right]. \tag{6}$$

For clusters with temperatures above about 8 keV, relativistic corrections also become significant. Analytic and fitting relations for the relativistic corrections to the SZ effect have been worked out by several groups: Challinor & Lasenby (1998), Itoh, Kohyama & Nozawa (1998) and Sazonov & Sunyaev (1998). Using the analytical formulae of Challinor & Lasenby (1998) up to second order, we determine the relativistic correction factor χ that needs to be applied to each summand of (6), so that $\Delta y_i \rightarrow \chi(T_i)\Delta y_i$.

2.2.2 Extrapolation of the temperature and gas density profiles

In the case of the *Chandra* X-ray Observatory, the detector size and the particle background limit the regions of clusters for which direct temperature measurements can be made ($r \leqslant r_1$) to a fraction of the virial radius. In order to calculate the predicted Comptonization parameter precisely, we need to extrapolate the temperature and electron density profiles out to the edge of the cluster, r_2 – or at least past the point where significant contributions to $y(r)$ are made. Here, for convenience, we will set $r_1 = r_{2500}$ and $r_2 = r_{200}$ (corresponding to the radii within which the mean enclosed mass density is $\Delta = 2500$ and $\Delta = 200$ times the critical density of the Universe, $\rho_\mathrm{crit}(z)$,

[1] Uncertainties in the determination of the distance scale associated with the assumption of isothermality were previously discussed by, e.g. Inagaki, Suginohara & Suto (1995) and Yoshikawa, Itoh & Suto (1998).

at redshift z, respectively). r_{2500} is typical of the outer radii for which useful information on the gas temperature profile can be obtained from *Chandra* observations. r_{200} is used to mark the outer edge of the cluster. (In Section 6 we shall show that the precise choice of r_2 does not affect the results significantly.)

We parametrize the total mass distributions in the clusters using a Navarro–Frenk–White (1995, NFW) model

$$\rho(r) = \frac{\rho_{\rm crit}(z)\,\delta_{\rm c}}{(r/r_{\rm s})\,(1+r/r_{\rm s})^2}, \tag{7}$$

where $\rho(r)$ is the mass density, $r_{\rm s}$ is the scale radius,

$$\rho_{\rm crit} = \frac{3H(z)^2}{8\pi G},$$

$H(z)$ is the Hubble constant, G is the gravitational constant,

$$\delta_{\rm c} = \frac{200}{3}\frac{c^3}{\ln(1+c) - c/(1+c)},$$

and c is the concentration parameter with $c = r_{200}/r_{\rm s}$.

The temperature $T(r_1)$, electron density $n_{\rm e}(r_1)$, and gas mass-weighted temperature $T_{{\rm m},r_1}$ within r_1 are assumed to be known from direct spatially resolved spectroscopy. We extrapolate the electron density from r_1 to r_2 using a power-law model $n_{\rm e}(r) \sim r^{-\gamma}$. The hydrostatic equation is then used to determine the temperature solution $T(r)$ for that power-law electron density profile in the given NFW potential (see Appendix A).

We fit the exponent γ of the electron density profile so that the model complies with two fixed quantities:

(i) the observed temperature $T(r_1)$ at r_1;
(ii) the *gas-mass* weighted temperature $T_{{\rm m},r_2}$ at r_2.

The power-law model approximates the true electron density profile between r_1 and r_2. (It is assumed that the galaxy cluster ends at r_2.) To determine the gas-mass weighted temperature $T_{{\rm m},r_2}$ within r_2, we use the Lokas & Mamon (2001) solution for the radial dependence of the ratio of kinetic energy $W_{\rm kin}$ and potential energy $W_{\rm pot}$ in an NFW potential with an isotropic velocity dispersion. The key assumption here is that the gas-mass weighted temperature $T_{{\rm m},r}$ inside a radius r is proportional to the kinetic energy of the mass distribution inside this radius (e.g. Eke, Navarro & Frenk 1998). We then calculate the change, q, of the ratio $W_{\rm kin}/W_{\rm pot}$ between r_1 and r_2 as

$$q = \frac{W_{\rm kin}(r_1)/W_{\rm pot}(r_1)}{W_{\rm kin}(r_2)/W_{\rm pot}(r_2)} = \frac{T_{{\rm m},r_1}/\left[M_{\rm tot}(r_1)/r_1\right]}{T_{{\rm m},r_2}/\left[M_{\rm tot}(r_2)/r_2\right]}, \tag{8}$$

where $M_{\rm tot}(r)$ is the total enclosed mass within radius r. The quantity q can be computed as a function of the scale radius $r_{\rm s}$ and the concentration parameter c of the NFW profile using the analytical formulae included in Appendix B.

Thus, given both the gas-mass weighted temperature $T_{{\rm m},r_1}$ at r_1 and a specific NFW mass model from the *Chandra* data, the gas-mass weighted temperature $T_{{\rm m},r}$ at r_2 can be obtained from equation (8). For the correct electron density slope γ, this is equal to the temperature that follows from the temperature solution (equation A3) and gas density profile $\rho_{\rm g}(r)$ [for which we assume $\rho_{\rm g}(r) = 1.1345\,m_{\rm p}\,n_{\rm e}(r)$] via the integral

$$T_{{\rm m},r_2} = \frac{1}{M_{{\rm g},r_2}}\left(M_{{\rm g},r_1}T_{{\rm m},r_1} + 4\pi\int_{r_1}^{r_2} T(r)\rho_{\rm g}(r)r^2\,{\rm d}r\right), \tag{9}$$

where $M_{{\rm g},r}$ is the gas mass inside the radius r.

We note that in cases where the X-ray data only extend to radii $r_0 \ll r_{2500}$ (within which cooling and/or heating effects may have modified $T_{{\rm m},r0}$ significantly), one should extrapolate the gas density (Appendix A) from r_0 to r_{200}, use this extrapolation to estimate the gas temperature and density at $r_1 = r_{2500}$, and then apply equation (8) between r_{2500} and r_{200} as usual. (This is possible because the extrapolation recipe is attached continuously to the *Chandra* data so that $T_{{\rm m},r}$ can be calculated for any exponent γ of the electron density extrapolation, regardless of where we attach the extrapolation.) We show below that this approach leads to robust answers in the case of *Chandra* observations of Abell 478, where the data cover only a relatively small radial range.

3 APPLICATION TO PUBLISHED *CHANDRA* AND SZ OBSERVATIONS

In this section we apply our method to *Chandra* and SZ observations of three galaxy clusters: RX J1347.5–1145, Abell 1835 and Abell 478. The X-ray data were originally published by Allen, Schmidt & Fabian (2002), Schmidt et al. (2001) and Sun et al. (2003), respectively.

3.1 Analysis of the X-ray data

Inside the region accessible to *Chandra*, the deprojected temperature and electron density profiles for the X-ray gas can be determined directly (under the assumption of spherical symmetry) using the methods described by Allen, Ettori & Fabian (2001a) and Schmidt et al. (2001). These data are then used to calculate the 68 per cent (1σ) confidence region of NFW mass models that provide the best-fit to the *Chandra* data. The results on the NFW mass models for RX J1347.5–1145, Abell 1835 and Abell 478 are summarized in Table 1.

We have carried out the extrapolation procedure described in Section 2.2.2 for every mass model within the 68 per cent confidence region obtained for each cluster. The radii r_1 and r_2, the temperature T_{r_1}, the ratio q (equation 8) calculated using the formulae in Lokas & Mamon (2001) and the effective power-law exponent γ of the electron density distribution for the clusters are given in Table 2. In the case of Abell 478, the *Chandra* data do not extend beyond $r \sim 0.3\,h_{70}^{-1}$ Mpc (corresponding to an overdensity $\Delta = 8500$). Within this radius radiative cooling may have affected the observed temperature of the cluster gas. Following the instructions from Section 2.2.2 for such a case, the temperature profile and electron density profiles were extrapolated from r_{8500}, but the exponent γ was determined using equation (8) between r_{2500} and r_{200}.

The application of our extrapolation procedure leads to the temperature and electron density profiles shown in Fig. 1. In this figure, both the best-fitting profile and allowed range of models are shown. Note that the small scatter in the electron density profiles is a consequence of the small scatter in the luminosity profile derived from the *Chandra* data. The temperature profiles have been binned using a simple emission-weighting scheme.

For Abell 478, it is also possible to determine the power-law slope of the electron density distribution beyond r_1 using *ROSAT*

Table 1. Details of the *Chandra* NFW mass models.

Object	Redshift	c	$r_{\rm s}$ (Mpc)
RX J1347.5–1145	0.451	$6.34^{+1.61}_{-1.36}$	$0.37^{+0.18}_{-0.12}$
Abell 1835	0.2523	$4.21^{+0.53}_{-0.61}$	$0.55^{+0.18}_{-0.09}$
Abell 478	0.088	$3.88^{+0.28}_{-0.36}$	$0.61^{+0.12}_{-0.07}$

Table 2. Details of the cluster model extrapolation.

Object	r_1 (Mpc)	r_2 (Mpc)	$T(r_1)$ (keV)	T_{m,r_2} (keV)	$n_{\mathrm{e}}(r_1)$ 10^{-4} cm^{-3}	q	γ
RX J1347.5–1145	$0.73^{+0.08}_{-0.09}$	$2.34^{+0.40}_{-0.35}$	$12.13^{+1.46}_{-0.41}$	$9.69^{+1.18}_{-1.52}$	$8.44^{+0.82}_{-0.20}$	$1.25^{+0.06}_{-0.05}$	$2.50^{+0.97}_{-1.02}$
Abell 1835	$0.67^{+0.05}_{-0.03}$	$2.36^{+0.26}_{-0.18}$	$11.34^{+0.20}_{-0.49}$	$7.97^{+0.75}_{-0.63}$	$7.46^{+0.81}_{-0.47}$	$1.36^{+0.05}_{-0.04}$	$1.88^{+0.39}_{-0.20}$
Abell 478	$0.66^{+0.03}_{-0.02}$	$2.36^{+0.18}_{-0.11}$	$8.29^{+0.16}_{-0.21}$	$6.41^{+0.48}_{-0.32}$	$5.92^{+0.60}_{-0.77}$	$1.40^{+0.02}_{-0.04}$	$1.90^{+0.09}_{-0.05}$

observations (Allen 2000). Fitting the *ROSAT* data between 0.3 Mpc and 0.9 Mpc yields a slope of $\gamma = 1.84 \pm 0.07$. This result is consistent with our model predictions given the expected steepening of the profile beyond the limit of the *ROSAT* data.

Finally, we note that the power-law model used in extrapolating the density profile provides only an approximation to the density values at large radii. (The true profile will steepen with increasing radius.) However, the pressure profile – the relevant quantity for predicting the Comptonization parameter profile – should be predicted accurately by the extrapolation procedure over the full range of radii.

3.2 Combination with the SZ data

3.2.1 RX J1347.5–1145

Detections of the SZ effect in RX J1347.5–1145 were published by Pointecouteau et al. (2001, P01) at 142.9 GHz, Komatsu et al. (2001) at 21 GHz and 150 GHz and Reese et al. (2002, R02) at 30 GHz using the Diabolo, Nobeyama and Owens Valley Radio Observatory (OVRO) instruments, respectively. The Comptonization parameters of all groups are consistent with each other. We compare the *Chandra* prediction with the Diabolo detection, which

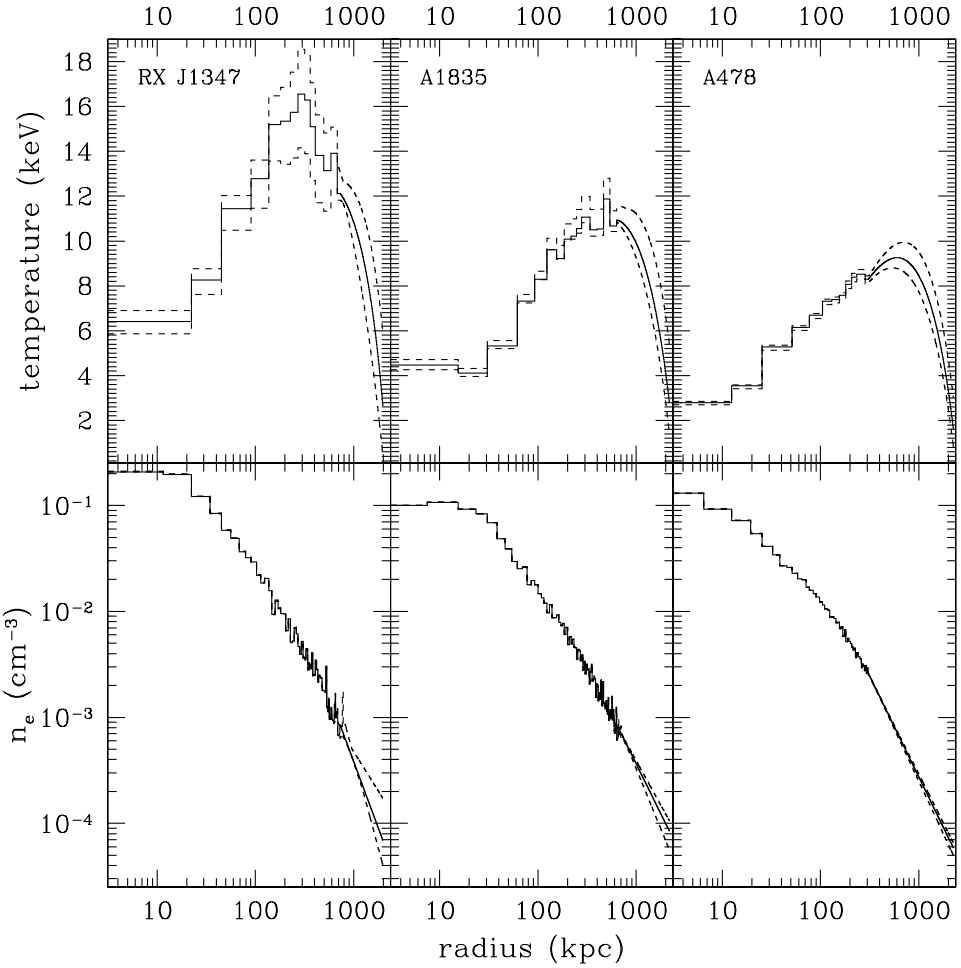

Figure 1. Extrapolated temperature and electron density profiles for RX J1347.5–1145, Abell 1835 and Abell 478. The best-fitting profiles are indicated by the solid lines. The upper and lower envelopes of the model ranges are plotted with dashed lines. For clarity we have only plotted the profiles up to the smallest $\Delta = 200$ overdensity radius of each model ensemble (see Table 2).

has the smaller beam size at 142.9 GHz of the two bolometers (Diabolo and Nobeyama), as well as a smaller error bar on the central Comptonization parameter than the OVRO interferometer result. P01 also published the flux decrement of the background radiation in four quadrants, which allows us to exclude the south-east quadrant, which contains hot, probably shocked, gas (Komatsu et al. 2001; Allen et al. 2002). Recently, Kitayama et al. (2004) have also carried out a detailed study of the intracluster medium in RX J1347.5–1145 using SZ observations. They obtain results in good agreement with those determined from the *Chandra* X-ray data.

In order to avoid the complicating effects of the shocked gas to the south-east of the cluster centre in RX J1347.5–1145, only data from the other three quadrants were used to determine the X-ray mass model (Allen et al. 2002). P01 published the flux decrements in the four quadrants, excluding a small square 16.2×16.2 arcsec^2 region around the nucleus (to avoid contamination by the central radio source). Adding all four quadrants, they find a flux decrement of $-(39.0 \pm 2.8)$ mJy in a square 100×100 arcmin^2 area around the cluster centre. However, this becomes $-(26.8 \pm 2.4)$ mJy once the south-east quadrant is excluded. This is the measurement we use for comparison with the X-ray data.

The intensity change ΔI due to the SZ effect can be calculated from the *Chandra* model. In the Kompaneets approximation (e.g. Birkinshaw 1999) this is given by

$$\Delta I = I_0\, y\, g(x) \tag{10}$$

where $I_0 = 2(k_{\rm B}\, T_0)^3/h^2\, c^2$,

$$g(x) = \frac{x^4 {\rm e}^x}{({\rm e}^x - 1)^2} \left[\frac{x({\rm e}^x + 1)}{{\rm e}^x - 1} - 4 \right], \tag{11}$$

and $x = h\nu/k_{\rm B}T_0$, with the Planck constant h, observing frequency ν and microwave background temperature T_0. Where relativistic corrections are significant, the Comptonization parameter y has to be modified appropriately (Section 2.2.1).

3.2.2 Abell 1835

The detection of the SZ effect in Abell 1835 was published by Mauskopf et al. (2000, M00) using the SuZIE I and SuZIE II bolometers. R02 have also published a detection using the OVRO interferometer at 30 GHz, which provides a consistent, but more precise determination of the Comptonization parameter. Here we compare our *Chandra* Comptonization profiles with the co-added SuZIE I scans published by M00, using their $\phi = -0.1$ arcsec offset of the X-ray cluster centre from the scan centre. To calculate their difference channels D3 (two beams separated by 4.6 arcmin) and T123 (triple beam chop of three beams separated by 2.3 arcmin) of the bolometer array we followed the description given by M00.

3.2.3 Abell 478

Abell 478 was observed by Myers et al. (1997) at 32 GHz and reanalysed by Mason et al. (2001, MMR). The observed decrement was published as an average y-parameter, $y = 7.52 \pm 0.56 \times 10^{-5}$, within the telescope beam. Note that we use their value without the relativistic correction, as we apply this correction to the X-ray model. We compare the observed SZ decrement with the *Chandra* prediction using the beam-switching technique described by Myers et al. (1997).

4 HUBBLE-CONSTANT DETERMINATION

The Comptonization parameter y defined in equation (3) depends upon the square root of the angular diameter distance to the cluster (Silk & White 1978; Cavaliere et al. 1979). By comparing the observed Comptonization parameter, $y_{\rm obs}$, within a given beam or aperture with the predicted value, $y_{\rm pred}$, from the X-ray data (for a given cosmology with $H_0 = 70\,{\rm km\,s^{-1}\ Mpc^{-1}}$), we can measure the Hubble constant, e.g. (MMR),

$$H_0 = \left(\frac{y_{\rm pred}}{y_{\rm obs}} \right)^2 \times 70\,{\rm km\,s^{-1}\,Mpc^{-1}}. \tag{12}$$

Since equation (10) is linear in the Comptonization parameter, these considerations also apply to the flux decrement $\Delta F_\nu = \omega \Delta I_\nu$ (Section 3.2), where ω is the solid angle of the emitting area, and ΔI_ν is the intensity decrement.

In order to compare our X-ray-predicted Comptonization parameter profiles with the direct SZ observations, we have convolved the X-ray profiles with the instrument beams for RX J1347.5–1145 [22 arcsec full width at half maximum (FWHM) beam] and Abell 478 (7.35 arcmin FWHM beam and 22.16 arcmin beam switching as described by Myers et al. 1997). For Abell 1835 we have added an additional normalization parameter to the NFW parameter space of scale radius and concentration parameter constrained by the *Chandra* data (Table 1). To determine the best-fitting value and 1σ error for this normalization parameter we added the χ^2 contribution from the SuZIE I co-added scans (1.7-arcmin FWHM beam and 2.3-arcmin or 4.6-arcmin beam separation) to the χ^2 contribution from the *Chandra* data. The normalization parameter directly measures the distance scale and is represented here by the resulting Hubble constant.

The results for the three galaxy clusters are shown in Table 3. For quantities with two-sided error bars, the root-mean-square error was used to determine the error on the Hubble constant. The weighted mean of the three Hubble-constant determinations in Table 3 is $H_0 = 69 \pm 8\,{\rm km\,s^{-1}\,Mpc^{-1}}$.

5 COMPARISON WITH THE β-MODEL AND PREVIOUS STUDIES

As the method for calculating the predicted Comptonization profiles presented here is significantly different from the standard isothermal β-model approach, it is instructive to compare the results on $y(r)$ and the Hubble constant obtained with the two approaches.

We have fitted the *Chandra* surface brightness profiles with a β-model (equation 1) inside a radius of 2.5 arcmin for RX J1347.5–1145, 3 arcmin for Abell 1835, and between radii of 1.5 arcmin and 4.5 arcmin for Abell 478. Note that in the case of Abell 478 the core of the cluster had to be excluded, because the central surface brightness profile is not flat, as is required by the β-model. The mean, emission-weighted temperatures from single-temperature fits to the *Chandra* spectra and the β-model parameters are given in Table 4. The temperatures were determined using the MEKAL (Kaastra & Mewe 1993; Liedahl et al. 1995) plasma model. The gas density normalization $n_{\rm e0}$ was calculated from the surface brightness using the MEKAL plasma emission model with the spectroscopically determined metallicities. Relativistic corrections were applied as described in Section 2.2.1. Using equation (5), together with the appropriate relativistic corrections factors, we obtain the central Comptonization parameters $y_0 = 1.13 \times 10^{-3}$ for RX J1347.5–1145, $y_0 = 4.2 \times 10^{-4}$ for Abell 1835 and $y_0 = 3.5 \times 10^{-4}$ for Abell 478.

Table 3. Results: Column 2 lists the observed quantity used to measure the Hubble constant. Columns 3 and 4 contain the measured and predicted values. The fifth column lists the observed areas. Column 6 contains the implied Hubble constant ($\Omega_{\rm m} = 0.3$, $\Omega_\Lambda = 0.7$).

Object	Quantity	Observed	Predicted	Area	H_0 [km s^{-1} Mpc^{-1}]
RX J1347.5–1145	ΔF_ν[mJy]	-26.8 ± 2.4 mJy	-25.5 ± 2.3 mJy	3 quadrants	63.4 ± 16.1
Abell 1835	SuZIE I scan	direct fit		24 arcmin scan	77.5 ± 16.5
Abell 478	$\bar{y}$ [10^{-5}]	7.52 ± 0.56	$7.43^{+0.12}_{-0.14}$	7.35 arcmin FWHM beam	68.3 ± 10.5

Table 4. β-model fits to the *Chandra* data.

Object	T (keV)	$\theta_{\rm c}$ (arcsec)	$n_{\rm e0}$ (cm^{-3})	β
RX J1347.5–1145	12.2	4.8	0.207	0.57
Abell 1835	8.1	9.0	0.100	0.61
Abell 478	6.8	26.6	0.068	0.55

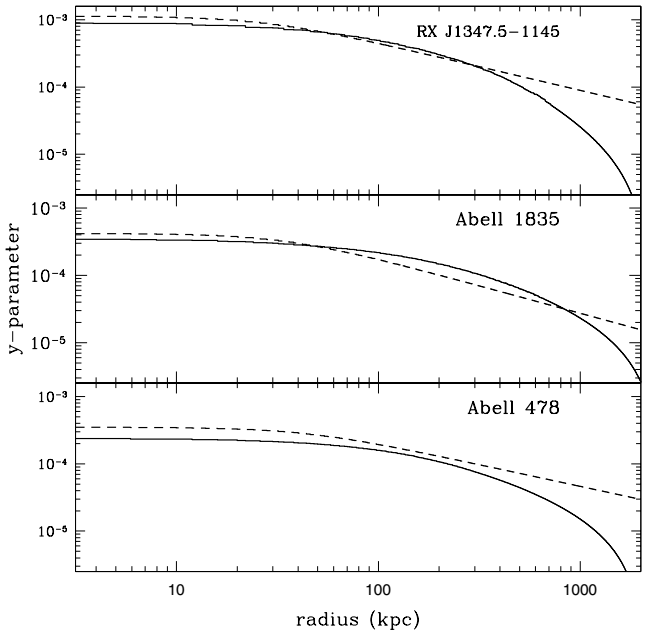

Figure 2. Best-fitting fully deprojected and extrapolated *Chandra* Comptonization parameter profiles (solid lines). The results from β-model fits to the *Chandra* data are plotted with dashed lines. All profiles are calculated for $H_0 = 70\,{\rm km\,s^{-1}\,Mpc^{-1}}$, $\Omega_{\rm m} = 0.3$ and $\Omega_\Lambda = 0.7$.

Fig. 2 shows the best-fitting Comptonization parameter profiles determined with our new method (solid line) together with the results from the standard isothermal β-model approach (dashed line). This plot shows that the Comptonization parameter profiles for the β-model differ substantially from the profiles obtained using the new, deprojected/extrapolated solution. First, the overall normalization in the core can be quite different. Secondly, the slope of the β-model is too shallow at large radii due to the infinite extent assumed in that model. [We note that the β-model can yield significantly different answers when applied to other data sets covering different ranges of radii (Mason et al. 2001; Pointecouteau et al. 2001; Reese et al. 2002). Here we have applied the two approaches to the same *Chandra* data simply to enable a direct comparison of the methods on the basis of the same, well-defined data sets.]

Applying the procedure described in Section 4 to the measured β-profile parameters yields Hubble constant estimates of $H_0 = 32\,{\rm km\,s^{-1}\,Mpc^{-1}}$ for RX J1347.5–1145, $H_0 = 29\,{\rm km\,s^{-1}\,Mpc^{-1}}$ for Abell 1835 and $H_0 = 103\,{\rm km\,s^{-1}\,Mpc^{-1}}$ for Abell 478. One can immediately see that the application of the isothermal β-model does not yield a consistent estimate when applied naively to *Chandra* data for the present sample of clusters.

It is also interesting to compare these estimates with previously published β-model estimates for the clusters discussed here. We have translated the electron densities from other studies into our assumed cosmology ($\Omega_{\rm m} = 0.3$, $\Omega_\Lambda = 0.7$ and $H_0 = 70\,{\rm km\,s^{-1}\,Mpc^{-1}}$).

RX J1347.5–1145: P01 determined a Hubble constant $H_0 = 44 \pm 6\,{\rm km\,s^{-1}\,Mpc^{-1}}$ using a $kT = 9.3$ keV isothermal model with the β-model parameters $\theta_{\rm c} = 8.4$ arcsec, $\beta = 0.56$ and $n_{\rm e0} = 0.102$ cm^{-3} from *ROSAT* (Schindler et al. 1997). Using the same temperature and a slightly different β-model, R02 found an angular diameter distance that implies $H_0 = 68.2^{+26.7}_{-15.8}\,{\rm km\,s^{-1}\,Mpc^{-1}}$. This estimate is consistent with the value we obtain using our fully deprojected and extrapolated cluster model (Table 3). However, the gas temperature and the other β-model parameters used by R02 are not consistent with the β-model parameters from *Chandra* (Table 4).

Abell 1835: For this cluster, M00 measured a Hubble constant $H_0 = 66^{+38}_{-22}\,{\rm km\,s^{-1}\,Mpc^{-1}}$ for a $kT = 9.8$ keV isothermal model with the β-model parameters $\theta_{\rm c} = 13.2$ arcsec, $\beta = 0.58$ and $n_{\rm e0} = 0.058$ cm^{-3} from a fit to *ROSAT* data. This temperature was obtained by allowing for a cooling flow component in the core of the cluster. R02 obtained an angular diameter distance to the cluster which implies $H_0 = 55.4^{+13.2}_{-8.8}\,{\rm km\,s^{-1}\,Mpc^{-1}}$, based on a $kT = 8.21$ keV isothermal model (no cooling flow correction). The difference between these two measurements can be attributed to the different isothermal temperatures and small differences in the assumed β-model parameters. Note also that the β-model parameters used in these studies are significantly different from those determined from *Chandra* (Table 4) over a smaller range of radii. This explains the difference in the predicted Hubble constant. However, the M00 result is consistent with the result we obtain from the deprojected and extrapolated X-ray data, which shows that it is possible to correct the β-model partially in the central region of the cluster when the surface brightness profile observed with the *ROSAT* field of view is used. For larger radii this approximation will fail, however, because of the fixed β-model slope.

Abell 478: MMR measured a Hubble constant $H_0 = 61^{+33}_{-21}\,{\rm km\,s^{-1}\,Mpc^{-1}}$ assuming an isothermal $kT = 8.4$ keV model with the β-model parameters $\theta_{\rm c} = 1$ arcmin, $\beta = 0.64$ and $n_{\rm e0} = 0.023$ cm^{-3} from *ROSAT*. This temperature also accounts for the presence of a cooling flow in the cluster core. Sun et al. (2003) improved upon the result by MMR by determining the Comptonization parameter as a function of radius from a deprojection of the *Chandra* data, and by extrapolating the *Chandra* data with a β-model based on a fit to the combined surface brightness profile from *Chandra* and *ROSAT*.

They used $\beta = 0.68$ and obtained a Hubble constant estimate $H_0 = 64^{+32}_{-18}\,\mathrm{km\,s^{-1}\,Mpc^{-1}}$, which lies between our value and the one obtained by MMR.

6 SUMMARY AND DISCUSSION

We have presented a new method for extrapolating the pressure profiles of galaxy clusters beyond the region accessible to current X-ray satellites such as *Chandra* and *XMM–Newton*, for use in combined X-ray and SZ studies. Our method assumes hydrostatic equilibrium, an NFW mass profile for the clusters and predicts the temperature profile and an effective power-law slope of the electron density profile. The method does not assume isothermality and provides a simple extrapolation recipe that can be easily implemented. We have applied our method to the *Chandra* data for three X-ray-bright, dynamically relaxed galaxy clusters, RX J1347.5–1145, Abell 1835 and Abell 478, and have obtained detailed temperature, electron density and Comptonization parameter profiles for these clusters out to the virial radius.

Since all three clusters have published SZ detections, we were also able to measure the Hubble constant for each, as shown in Table 3. The individual measurements are consistent with each other and yield a weighted mean of $H_0 = 69 \pm 8\,\mathrm{km\,s^{-1}\,Mpc^{-1}}$. This result is consistent with findings from the Hubble Key Project ($H_0 = 72 \pm 8\,\mathrm{km\,s^{-1}\,Mpc^{-1}}$; Freedman et al. 2001) and combined studies of the cosmic microwave background and X-ray galaxy cluster data ($H_0 = 68.4^{+2.0}_{-1.4}\,\mathrm{km\,s^{-1}\,Mpc^{-1}}$; Allen, Schmidt & Bridle 2003). Note that our weighted mean value does not include additional systematical errors, due to, e.g. clumping or asphericity, although for such regular, relaxed clusters these should be at a minimum.

The contribution to the predicted Comptonization parameter from material beyond the regions directly observed with *Chandra*, modelled by our extrapolation procedure, varies from system to system. For RX J1347.5–1145 the correction to the Comptonization parameter in the region used in Table 3 amounts only to 1 per cent and is negligible. For Abell 1835, however, the contribution from material in the extrapolated region amounts to 20 per cent, and for Abell 478 the contribution rises to 68 per cent. This shows that a robust extrapolation method is necessary when combining X-ray and SZ observations to infer cosmological information.

We have estimated the effect of changing the outer radius r_{200} by repeating the calculation for Abell 478, but stopping at r_{500}. This leads to a 4.2 per cent smaller average Comptonization parameter, well within the observational error bar.

We have compared the Comptonization parameter profiles predicted by our method with the profiles obtained by fitting an isothermal β-model to the *Chandra* data. We find that a naive application of the β-model approach leads to profiles with significantly different central Comptonization parameters and predicts different slopes for the Comptonization parameter profiles at large radii. The isothermal β-model also leads to inconsistent Hubble constant estimates when applied to the *Chandra* data sets considered here.

It is clear that for galaxy clusters like Abell 478, a field of view larger than the one afforded by the *Chandra* ACIS-S3 detector would be beneficial. In this respect the combination of *Chandra* and *XMM–Newton* observations will help (e.g. Pointecouteau et al. 2004), although the detector background will still prohibit precise measurements of the temperature profile beyond $r \sim 0.5 r_{200}$. (We also note that the high spatial resolution of *Chandra* is important in resolving the central temperature profile and constraining the best-fitting NFW mass models.)

Observations for a larger sample of clusters, as well as deeper X-ray and SZ observations, should make this a powerful method to explore the cosmological distance scale. In the first case, it will be important to concentrate such studies on the largest, dynamically relaxed clusters for which systematic uncertainties associated with the deprojection method and assumption of hydrostatic equilibrium are at a minimum.

ACKNOWLEDGMENTS

We thank Y. Suto, N. Itoh and the anonymous referee for comments. We thank the developers of the GNU Octave numerical computation language and the GNU Scientific Library for these tools. SWA and ACF acknowledge the support of the Royal Society.

REFERENCES

Allen S. W., 2000, MNRAS, 315, 269
Allen S. W., Ettori S., Fabian A. C., 2001a, MNRAS, 324, 877
Allen S. W., Schmidt R. W., Fabian A. C., 2001b, MNRAS, 328, L37
Allen S. W., Schmidt R. W., Fabian A. C., 2002, MNRAS, 335, 256
Allen S. W., Schmidt R. W., Bridle S. L., 2003, MNRAS, 346, 593
Birkinshaw M., 1999, Phys. Rep., 310, 97
Carlstrom J. E., Joy M., Grego L., Holder G., Holzapfel W. L., LaRoque S., Mohr J. J., Reese E. D., 2001, in Durret F., Gerbal G., eds, Proc. IAP Conf., Constructing the Universe with Clusters of Galaxies (astro-ph/0103480)
Cavaliere A., Fusco-Femiano R., 1978, A&A, 70, 677
Cavaliere A., Danese L., de Zotti G., 1979, A&A, 75, 322
Challinor A., Lasenby A., 1998, ApJ, 499, 1
Eke V. R., Navarro J. F., Frenk C. S., 1998, ApJ, 503, 569
Freedman W. L. et al., 2001, ApJ, 553, 47
Gradshteyn I. S., Ryzhik I. M., 2000, Table of Integrals, Series and Products, 6th edn. Academic Press, San Diego
Inagaki Y., Suginohara T., Suto, Y., 1995, PASJ, 47, 411
Itoh N., Kohyama Y., Nozawa S., 1998, ApJ, 502, 7
Jones M. E. et al., 2001, MNRAS, submitted (astro-ph/0103046)
Kaastra J. S., Mewe R., 1993, Legacy, 3, 16
Kaastra J. S. et al., 2004, A&A, 413, 415
Kitayama T., Komatsu E., Ota N., Kuwabara T., Suto Y., Yoshikawa K., Hattori M., Matsuo H., 2004, PASJ, 56, 17
Komatsu E. et al., 2001, PASJ, 53, 57
Liedahl D. A., Osterheld A. L., Goldstein W. H., 1995, ApJ, 438, L115
Lokas E. L., Mamon G. A., 2001, MNRAS, 321, 155
Mason B. S., Myers S. T., Readhead A. C. S., 2001, ApJ, 555, L11 (MMR)
Mauskopf P. D. et al., 2000, ApJ, 538, 505 (M00)
Myers S. T., Baker J. E., Readhead A. C. S., Leitch E. M., Herbig T., 1997, ApJ, 485, 1
Navarro J. F., Frenk C. S., White S. D. M., 1995, MNRAS, 275, 720 (NFW)
Pointecouteau E., Giard M., Benoit A., Désert F. X., Bernard J. P., Coron N., Lamarre J. M., 2001, ApJ, 552, 42 (P01)
Pointecouteau E., Arnaud M., Kaastra J., de Plaa J. 2004, A&A, in press (astro-ph/0403596)
Reese E. D., Carlstrom J. E., Joy M., Mohr J. J., Grego L., Holzapfel W. L., 2002, ApJ, 581, 53 (R02)
Sarazin C. L., 1988, X-ray Emission from Clusters of Galaxies. Cambridge Univ. Press, Cambridge
Sazonov S. Y., Sunyaev R. A., 1998, ApJ, 508, 1
Schindler S., Hattori M., Neumann D. M., Boehringer H., 1997, A&A, 317, 646
Schmidt R. W., Allen S. W., Fabian A. C., 2001, MNRAS, 327, 1057
Silk J., White S. D. M., 1978, ApJ, 226, L103
Sun M., Jones C., Murray S. S., Allen S. W., Fabian A. C., Edge A. C., 2003, ApJ, 587, 619
Sunyaev R., Zeldovich Y., 1972, Comments Astrophys. Space Phys., 4, 173
Yoshikawa K., Itoh M., Suto Y., 1998, PASJ, 50, 203

APPENDIX A: AN EXTRAPOLATION SOLUTION FOR THE X-RAY GAS TEMPERATURE PROFILE IN AN NFW POTENTIAL

Let the mass distribution of a galaxy cluster be parametrized by an NFW mass model (equation 7). Also, let the electron density distribution for a certain range of radii be parametrized by a power-law model

$$n_{\rm e}(r) \sim r^{-\gamma}. \tag{A1}$$

The temperature as a function of radius can then be determined under the assumption of hydrostatic equilibrium by solving the hydrostatic equation

$$\frac{1}{n_{\rm e}}\frac{{\rm d}(n_{\rm e}\,kT)}{{\rm d}r} = -\mu m_{\rm p}\frac{GM}{r^2}, \tag{A2}$$

where k is the Boltzmann constant, $\mu = 0.60$ is the molecular weight of the gas and $m_{\rm p}$ is the proton mass (note that the normalization of (A1) drops out of this equation). Using the method of the variation of the constant one finds that is possible to write the solution of (A2) in the form

$$\begin{aligned} kT(r) = \left(\frac{r}{r_1}\right)^{\gamma}\Bigg\{ & kT_1 - \frac{4\pi r_{\rm s}^2\delta_{\rm c}\rho_{\rm c}\mu m_{\rm p}G}{(1+\gamma)\,r_1 r^{1+\gamma}} \\ & \times\Bigg[r\,r_1^{1+\gamma}\,{}_2F_1\left(-\gamma, 1; 1-\gamma; -\frac{r}{r_{\rm s}}\right) \\ & - r_1\,r^{1+\gamma}\,{}_2F_1\left(-\gamma, 1; 1-\gamma; -\frac{r_1}{r_{\rm s}}\right) \\ & - r_{\rm s}r_1^{1+\gamma}\ln\left(1+\frac{r}{r_{\rm s}}\right) + r_{\rm s}r^{1+\gamma}\ln\left(1+\frac{r_1}{r_{\rm s}}\right)\Bigg]\Bigg\}, \end{aligned} \tag{A3}$$

with the boundary condition $T(r_1) = T_1$. ${}_2F_1$ is the hypergeometric function (e.g. Gradshteyn & Ryzhik 2000, p. 995) which is well-defined on the whole negative real axis and is available in standard mathematical packages.

APPENDIX B: THE ENERGY DISTRIBUTION OF THE NFW MASS DISTRIBUTION

In this Appendix we list the Lokas & Mamon (2001) expressions for the potential energy $W_{\rm pot}$ and the kinetic energy $W_{\rm kin}$ in an NFW potential with an isotropic velocity dispersion, as a function of radius r. The ratio of these quantities is used in Section 2.2.2 to determine the cluster model extrapolation. It can be calculated from the concentration parameter c and the scale radius $r_{\rm s}$.

The radial dependence of the potential energy associated with an NFW mass distribution with virial radius $r_{200} = cr_{\rm s}$ as a function of (scaled) radius $s = r/r_{200}$ is

$$W_{\rm pot}(s) = -W_\infty\left[1 - \frac{1}{(1+cs)^2} - \frac{2\ln(1+cs)}{1+cs}\right] \tag{B1}$$

(equation 21 in Lokas & Mamon 2001), where W_∞ is the asymptotic value

$$W_\infty = \frac{GM_{\rm tot}^2(r_{200})}{2r_{\rm s}[\ln(1+c) - c/(1+c)]^2}. \tag{B2}$$

The radial dependence of the kinetic energy, assuming isotropic velocity dispersion, is

$$\begin{aligned} W_{\rm kin}(s) = \frac{1}{2}W_\infty\Bigg\{ & -3 + \frac{3}{1+cs} - 2\ln(1+cs) \\ & + cs[5 + 3\ln(1+cs)] - c^2s^2[7 + 6\ln(1+cs)] \\ & + c^3s^3[\pi^2 - \ln c - \ln s + \ln(1+cs) \\ & + 3\ln^2(1+cs) + 6{\rm Li}_2(-cs)]\Bigg\} \end{aligned} \tag{B3}$$

(equation 24 in Lokas & Mamon 2001), where $\rm Li_2$ is the dilogarithm.

This paper has been typeset from a TEX/LATEX file prepared by the author.